

# Hydrogen production by partial oxidation of methanol over Au/CuO/ZnO catalysts

Hsien-Chang Yang, Feg-Wen Chang\*, L. Selva Roselin

*Department of Chemical and Materials Engineering, National Central University, Chungli 32001, Taiwan*

Received 7 August 2006; received in revised form 25 June 2007; accepted 3 July 2007

Available online 10 July 2007

## Abstract

Hydrogen production by partial oxidation of methanol (POM) ( $\text{CH}_3\text{OH} + 0.5\text{O}_2 \rightarrow 2\text{H}_2 + \text{CO}_2$ ) was examined over Au/CuO/ZnO (Au 3 wt.%, Cu 37 wt.% and Zn 60 wt.%) catalysts, prepared by the co-precipitation method. The activity of Au/CuO/ZnO catalysts has been compared with that of CuO/ZnO (Cu 40 wt.% and Zn 60 wt.%) catalysts. The catalysts were characterized by XRD, TEM and TPR analyses. The Au/CuO/ZnO catalysts are more active and exhibit higher hydrogen selectively with smaller amount of CO compared to the CuO/ZnO catalysts. The enhanced activity of Au/CuO/ZnO catalyst is due to the strong interaction between Au and CuO species as evidenced by TPR analysis. The influence of calcination temperature on the catalytic activity of Au/CuO/ZnO catalyst depends on crystalline phases of support and particle size of Au and CuO present on the catalysts. The optimum calcination temperature is 573 K. The catalytic performance at various reaction temperatures shows that at 448 K the reaction sets on with  $\text{O}_2$  completely consumed. A high hydrogen selectivity of 97.7% is attained at 523 K with 100% methanol conversion. The undesired by-product, CO is formed in very small amount throughout the temperature range studied.

© 2007 Elsevier B.V. All rights reserved.

**Keywords:** Gold catalyst; Copper oxide; Zinc oxide; Partial oxidation of methanol; Hydrogen

## 1. Introduction

Hydrogen production by partial oxidation of methanol (POM) is of great interest for the development of fuel cell (proton exchange membrane fuel cell, PEMFC). Hydrogen-powered fuel cells generate electricity much more efficiently than fossil fuel without discharging any polluting by-products such as  $\text{NO}_x$ ,  $\text{SO}_x$ , etc. [1,2]. Previous studies on POM to produce hydrogen showed that Cu-based catalysts such as Cu/ZnO and Cu/ZnO/ $\text{Al}_2\text{O}_3$  were active [3–7]. Unfortunately, these catalysts produce considerable amount of carbon monoxide as a by-product. CO is a poison to fuel cell anodes. If the carbon monoxide level exceeds a few ppm, the precious metal-based anode electrocatalyst of the fuel cell is deactivated. The discovery of the exceptionally high activity of supported Au catalysts for low temperature CO oxidation [8,9] aroused interest in testing these catalysts for POM to produce hydrogen. Our previous investigation on POM showed that Au/ $\text{TiO}_2$  catalyst was active for selective formation of hydrogen [10]. Since the catalytic

activity and stability of the Au/ $\text{TiO}_2$  system is not high enough, modification of the catalyst for improved activity and stability is needed. Our recent report has proved that the catalytic activity and stability of supported gold catalysts for hydrogen generation is improved by using a composite support [11]. Even though the catalytic activity and stability of the gold catalyst was improved by using the composite support, further improvement in the activity is necessary. In the present work, the catalytic activity of Au/CuO/ZnO catalysts has been studied for the formation of hydrogen by POM using oxygen as oxidant. The catalyst characterizations included are X-ray diffraction (XRD), transmission electron microscopy (TEM) and temperature-programmed reduction (TPR). Attention has been paid to the optimization of calcination temperature and reaction temperature in order to achieve complete conversion of methanol for the selective formation of hydrogen.

## 2. Experimental

### 2.1. Catalyst preparation

The weight percentage of each metal in the most active CuO/ZnO catalysts for POM reported earlier is 40 wt.% Cu and

\* Corresponding author. Tel.: +886 3 4227151x34202; fax: +886 3 4252296.  
E-mail address: [fwchang@cc.ncu.edu.tw](mailto:fwchang@cc.ncu.edu.tw) (F.-W. Chang).

60 wt.% Zn [3]. Therefore, the CuO/ZnO catalysts with the same composition were prepared in this study. For Au/CuO/ZnO catalysts, the weight percentages of Au, Cu and Zn were fixed as 3, 37 and 60 wt.%, respectively. The Au/CuO/ZnO catalysts were prepared by the co-precipitation method [9]. Typically, an aqueous solution of  $\text{Cu}(\text{NO}_3)_2 \cdot 2.5\text{H}_2\text{O}$  (0.25 M),  $\text{Zn}(\text{NO}_3)_2$  (0.25 M), and  $\text{HAuCl}_4$  (0.1 M) (Fluka) were mixed together in a volume ratio of 1.5:2.4:0.1, with stirring, at 343 K. Aqueous  $\text{Na}_2\text{CO}_3$  (0.1 M) was added dropwise to the mixed nitrate solution until pH 8.5 was attained. The precipitate formed in this process was aged at 343 K for 2.5 h. The precipitate was recovered by filtration and washed with hot deionized water (343 K) until complete elimination of  $\text{Cl}^-$  and  $\text{Na}^+$  ions. Then the sample was dried in air at 373 K for 24 h to give a material designated as the catalyst precursor, which was subsequently calcined in air at different temperatures for 3 h. CuO/ZnO catalyst was prepared using similar preparation procedures.

## 2.2. Characterization

X-ray powder diffraction (XRD) patterns of the catalyst samples were obtained in an X-ray diffractometer (Bruker, Model D8A) operated at 40 kV and 40 mA using  $\text{Cu K}\alpha$  radiation with a wavelength of  $1.5406 \text{ \AA}$ , from  $5^\circ$  to  $80^\circ$  at a rate of  $0.05^\circ \text{ s}^{-1}$ .

Transmission electron microscopy (TEM) studies were performed on a JEOL TEM-2000FXII instrument operated at 160 kV. To obtain suitable samples for TEM characterization, the powders were dispersed in ethanol by ultrasonication. A drop of the solution was then deposited on to a thin carbon film supported on a copper microgrid and left to dry at 333 K. For each catalyst, about 100 Au particles were measured in order to determine a statistically justified average particle size and size distribution.

Temperature-programmed reduction (TPR) of the catalyst was performed in a U-shaped micro-reactor made of quartz, surrounded with a furnace controlled by a programmed heating system. Prior to the TPR experiment, 20 mg of the catalyst sample was pretreated under flowing Ar (20 ml/min) at 523 K for 45 min. After the pretreatment, the sample was cooled to room temperature. A reducing gas composed of 5%  $\text{H}_2$  plus 95% Ar was employed at a flow rate of 20 ml/min, with a heating ramp of 10 K/min from 373 to 773 K. The amount of the consumed  $\text{H}_2$  was determined by a thermal conductivity detector (TCD).

## 2.3. Catalytic activity

Partial oxidation of methanol (POM) was carried out using an apparatus, which has been described in detail elsewhere [10]. The reaction was carried out at atmospheric pressure and at temperatures between 423 and 548 K, using a U-shaped microreactor made of quartz (i.d. = 4 mm). The reactor was located in a temperature-programmable furnace with a type K thermocouple placed in the center of the catalyst bed. Typically, 20 mg of catalyst was used in each experiment. Methanol was fed into the pre-heater by means of a Cole-Parmer liquid pump (Model: 77120-30) at a rate of 0.924 ml/h. The oxygen and argon (diluent) flows were adjusted by Brooks 5850E mass flow controllers.

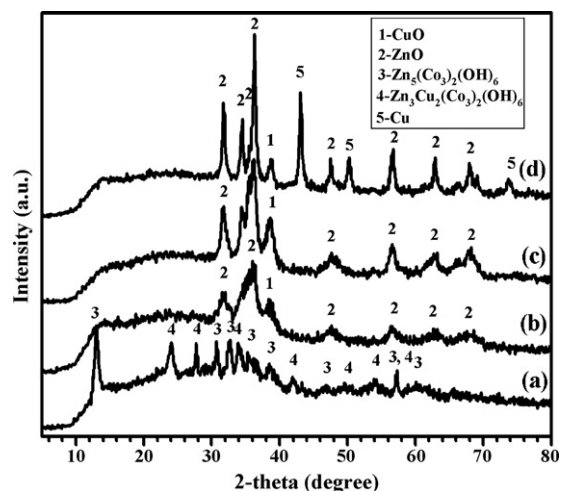


Fig. 1. XRD patterns of Au/CuO/ZnO catalysts before calcination, after calcination at different temperatures and after POM reaction: (a) uncalcined; (b) 573 K; (c) 673 K; (d) after POM reaction at 523 K for 2 h.

The total flow was 60 ml/min with the  $\text{O}_2/\text{CH}_3\text{OH}$  molar ratio of 0.5. The reaction products were analyzed on-line using two gas chromatographs (GC) equipped with thermal conductivity detector and porapak Q and carbosieve S-II columns.

## 3. Results and discussion

### 3.1. XRD

XRD was used to identify the crystalline phases present on the Au/CuO/ZnO catalysts before and after calcination at different temperatures. Fig. 1 shows the XRD patterns of Au/CuO/ZnO catalysts before and after calcination at 573 and 673 K. The pattern of the Au/CuO/ZnO catalyst calcined at 573 K after exposure to POM reaction at 523 K for 2 h is also inserted. The XRD of the uncalcined sample (Fig. 1a) exhibited the presence of hydrozincite ( $\text{Zn}_5(\text{CO}_3)_2(\text{OH})_6$ ) and aurichalcite ( $\text{Zn}_3\text{Cu}_2(\text{CO}_3)_2(\text{OH})_6$ ) compounds [3]. For example, the intense lines at  $2\theta = 13.0$ ,  $24.3$  and  $47.5$  are characteristic of hydrozincite and those at  $2\theta = 34.1^\circ$ ,  $41.9^\circ$  and  $50.1^\circ$  are characteristic of aurichalcite. The sample calcined at 573 K undergo thermal decomposition, resulting in the formation of a mixture of poorly crystallized CuO and ZnO phases as observed by the diminished peak intensities of the hydrozincite and aurichalcite compounds and appearance of peaks corresponding to ZnO and CuO (Fig. 1b). The crystallinity of the ZnO and CuO phases increased with increasing calcination temperature to 673 K (Fig. 1c). Fig. 1d illustrates the XRD patterns of Au/CuO/ZnO catalyst calcined at 573 K after POM at 523 K for 2 h. Upon reaction with methanol and oxygen at 523 K, the line characteristic of  $\text{Cu}^0$  appears at  $2\theta = 43.0^\circ$ . This can be interpreted to mean that CuO is reduced to metallic Cu during the reaction. Wang et al. [12] have also observed the reduction of CuO species in Cu/SiO<sub>2</sub> catalysts to metallic copper in a similar type of reaction. As seen from Fig. 1, for all the samples, the XRD analysis did not reveal the presences of any oxidic Au species ( $2\theta = 25.5^\circ$ ,  $30.2^\circ$  and  $32.5^\circ$ ) or metallic Au species ( $2\theta = 38.2^\circ$ ,  $44.4^\circ$  and

64.5°), suggesting that gold particles are highly dispersed on the surface, that the Au peaks are overlapped by hydrozincite and/or CuO, or that the corresponding gold particles are too small to be detected by the instrument. According to Chang et al. [13], the limitations of XRD for gold crystallites correspond to a particle size smaller than 5 nm. TEM technique was subsequently employed to confirm the Au particle size in the catalysts.

### 3.2. TEM

The particle size of gold and copper species and their level of dispersion on the support in Au/CuO/ZnO catalysts before and after calcination at different temperatures were examined by transmission electron microscope (TEM) study. Fig. 2 presents the TEM pictures of uncalcined and calcined Au/CuO/ZnO catalyst samples (573 and 673 K) and the sample calcined at 573 K

after exposure to POM. Fig. 2a shows the TEM image of the Au/CuO/ZnO catalyst before calcination. During the drying procedure, aurichalcite and the gold precursor thermally decomposed to a small extent to form CuO and metallic Au. Deposited gold particles appear as small black spots in the TEM photograph and are uniformly dispersed on the support. The gold and copper crystallites are sphere in shape with an average diameter of 2.5 and 6.2 nm, respectively. As shown in Fig. 2b, the TEM image of the Au/CuO/ZnO catalyst calcined at 573 K indicates an increase in the number of gold and copper crystallites. Zhang et al. [14] reported that in gold catalyst supported on zinc oxide, gold oxide species are decomposed to metallic gold when the sample was calcined at 513 K. Therefore during calcination, the gold precursor decomposed to metallic gold, and the hydrozincite and aurichalcite were decomposed to form CuO. In the figure, the large particles are CuO particles, which exhibited an

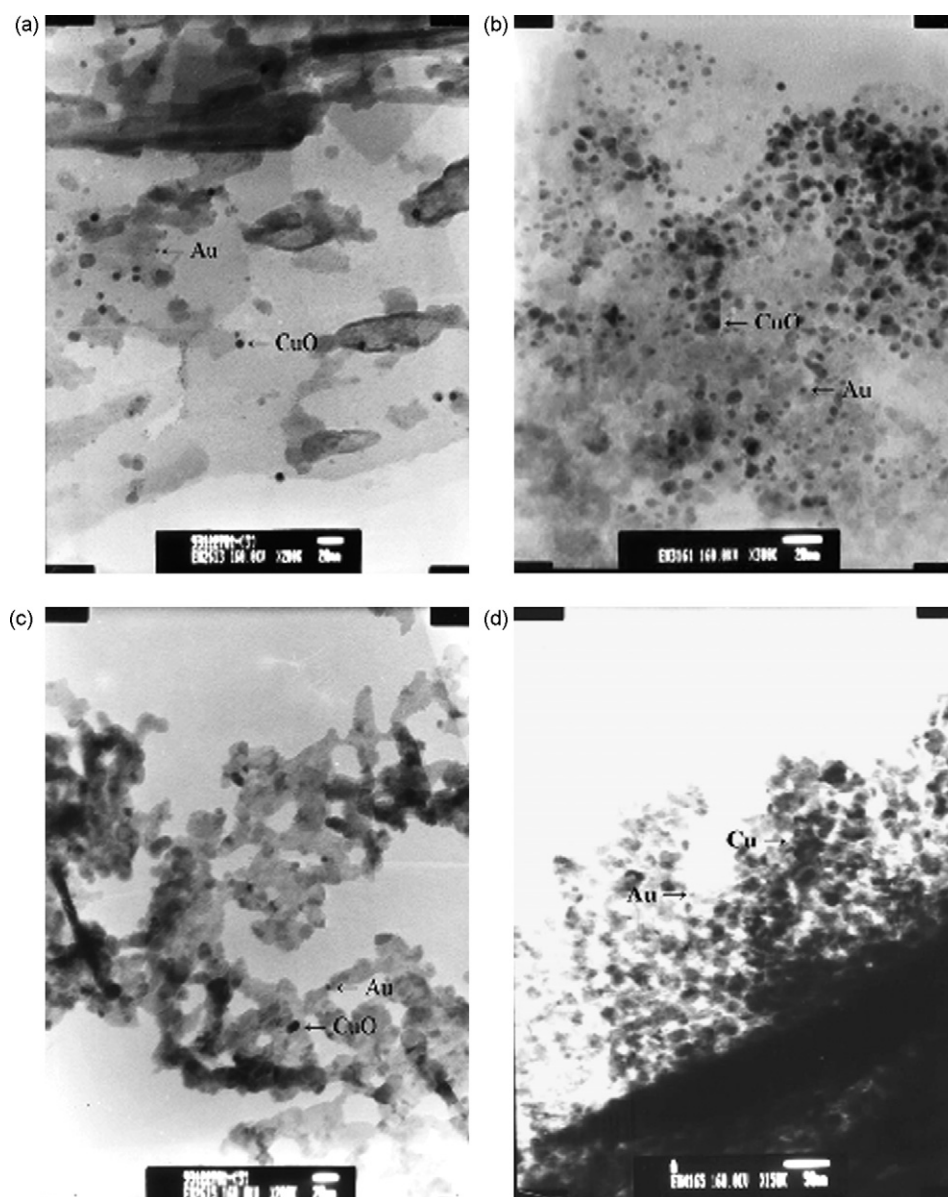


Fig. 2. TEM images of Au/CuO/ZnO catalysts before calcination, after calcination at different temperatures and after POM reaction: (a) uncalcined (200 $\times$ ); (b) 573 K (300 $\times$ ); (c) 673 K (200 $\times$ ); (d) after POM reaction at 523 K for 2 h (150 $\times$ ).

average diameter of 9.5 nm. The small gold particles appear to be fairly homogeneously distributed over the support and have an average diameter of 3.4 nm. This result clearly indicates that at higher calcination temperature both the size and the number of gold particles are increased. Fig. 2c shows the TEM image of the Au/CuO/ZnO catalyst calcined at 673 K. When the catalyst is calcined at 673 K, the gold and CuO particles grow to an average size of 4.6 and 13 nm, respectively. At this temperature, aggregation of copper particles becomes larger due to sintering and is accompanied by changes in their shape from a spherical to irregular shape. Therefore, at higher calcination temperature, gold and copper particles sinter, and so, the number of gold and copper crystallites is decreased. It implies that sintering of the catalyst takes place at 673 K; consequently, the number of active sites is decreased. Fig. 2d shows the TEM image of Au/CuO/ZnO catalyst calcined at 573 K after exposure to POM at 523 K for 2 h. The particle size of Au and Cu are increased from 3.4 to 5.4 nm and from 9.5 to 27 nm, respectively. The POM reaction results in the increase in the size of Au and Cu crystallites.

### 3.3. TPR

Fig. 3 illustrates the TPR patterns of Au/ZnO, CuO/ZnO and Au/CuO/ZnO catalysts calcined at 573 K. The Au/ZnO sample (Fig. 3a) does not exhibit any signal which indicates that gold is present only in a metallic state after calcination at 573 K, in agreement with previous reports [14]. The TPR pattern of CuO/ZnO (Fig. 3b) shows a major peak at 500 K along with two shoulder peaks at 460 and 525 K. The major peak at 500 K corresponds to the reduction of CuO to metallic copper. The low temperature shoulder peak at 460 K is assigned to the reduction of CuO to Cu<sup>+</sup> and the high temperature shoulder peak at 525 K is assigned to the reduction of Cu<sup>+</sup> to metallic copper [15–17]. The TPR pattern of the Au/CuO/ZnO sample (Fig. 3c) exhibits a broad peak with two unresolved signals at 486 and 500 K. The two TPR signals are related to the two step reduction (Cu(II) → Cu(I) → Cu(0)) as suggested by Fang et al. [18]. It is noteworthy that both the shape and reduction tem-

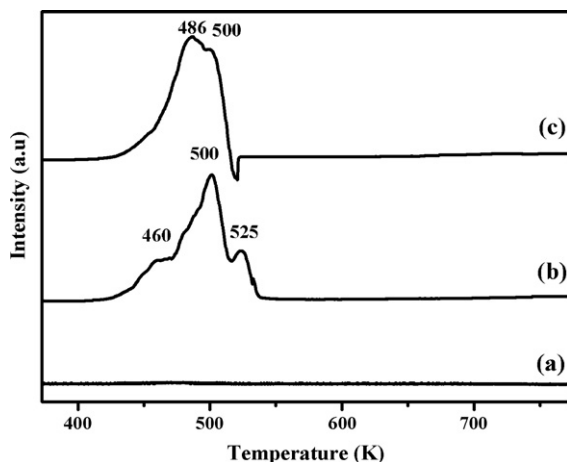


Fig. 3. TPR curves of Au/ZnO, CuO/ZnO and Au/CuO/ZnO catalysts calcined at 573 K: (a) Au/ZnO catalyst; (b) CuO/ZnO catalyst; (c) Au/CuO/ZnO catalyst.

perature for CuO in CuO/ZnO and Au/CuO/ZnO are different. The reduction peak of CuO in the Au/CuO/ZnO sample shifts to a lower temperature compared with the CuO/ZnO sample (Fig. 3b and c). This shows that Au promotes CuO reduction, which occurs at lower temperatures, in accordance with previous work [19]. Cabrera et al. [20] pointed out that metallic Pd exhibited a certain promotion effect on the CuO reduction in palladium–copper–zinc catalysts. The enhanced reducibility by the metal in the catalysts is reported in other catalysts [21–23]. Scirè et al. [22] have reported that reduction of Fe<sub>2</sub>O<sub>3</sub> enhanced by Au in Au/Fe<sub>2</sub>O<sub>3</sub> catalysts. The enhanced reducibility of Fe<sub>2</sub>O<sub>3</sub> has been explained in terms of ability to weaken the Fe–O bond. The metal in Fe<sub>2</sub>O<sub>3</sub> could lead to decrease in the strength of the Fe–O bond located nearby the metal atom [23]. Similar phenomenon is occurring here; the Cu–O bond is weakened by the presence of metal Au. Therefore, we may propose that there is some sort of interaction between Au and CuO in the Au/CuO/ZnO catalysts, which can enhance the reducibility of CuO.

### 3.4. Catalytic activity

The catalytic activity and product distribution in the partial oxidation of methanol (POM) over Au/CuO/ZnO catalysts were studied with an O<sub>2</sub>/CH<sub>3</sub>OH molar ratio of 0.5. Hydrogen and carbon dioxide were the main products, while water and carbon monoxide were the by-products. Methanol conversion, hydrogen and carbon monoxide selectivity are defined, respectively, as follows:

CH<sub>3</sub>OH conversion (%)

$$= (\text{moles of methanol consumed} / \text{moles of methanol fed}) \times 100,$$

H<sub>2</sub> selectivity (%)

$$= (\text{moles of H}_2 \text{ produced} / \text{moles of methanol consumed} \times 2) \times 100,$$

CO selectivity (%)

$$= (\text{moles of CO produced} / \text{moles of methanol consumed}) \times 100.$$

Fig. 4 shows the comparison of catalytic activity of CuO/ZnO and Au/CuO/ZnO catalysts for partial oxidation of methanol (POM) at 523 K. These two catalysts showed similar high methanol conversion (100%). However, they differ in their product distribution. The Au/CuO/ZnO catalysts displayed higher hydrogen selectivity with lower carbon monoxide selectivity compared to that over CuO/ZnO catalysts. The hydrogen selectivity is 97.7 and 84.6%, respectively for Au/CuO/ZnO and CuO/ZnO catalysts. It is interesting to note that the Au/CuO/ZnO catalyst produced negligible amount of CO. However, significant amount of CO was observed over CuO/ZnO catalysts, being consistent with the results reported in the previous studies on supported copper catalysts [3,24,25]. The CO selectivity

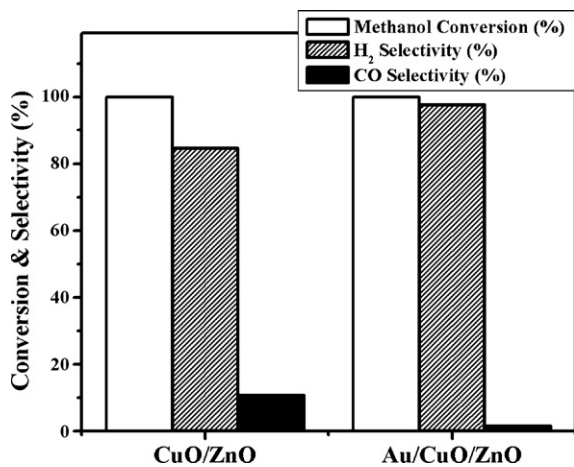


Fig. 4. Catalytic performance of CuO/ZnO and Au/CuO/ZnO catalysts for methanol conversion, hydrogen selectivity and carbon monoxide selectivity for partial oxidation of methanol (calcination temperature, 573 K; reaction temperature, 523 K; reaction time, 10 min).

over Au/CuO/ZnO and CuO/ZnO catalysts is 1.5 and 10.7%, respectively. In our recent studies on POM, we have shown that Au/TiO<sub>2</sub> and Au/TiO<sub>2</sub>-Fe<sub>2</sub>O<sub>3</sub> catalysts are active in producing hydrogen with small amount of CO [10,11]. Therefore, the enhanced activity of Au/CuO/ZnO catalyst to produce hydrogen with negligible amount of CO is due to the strong interaction between Au and CuO species as evidenced by TPR studies (Fig. 3b and c). In this catalyst, partial oxidation of methanol was mainly found to take place leading to high hydrogen and carbon dioxide selectivities. Moreover, Au/CuO/ZnO catalysts are reported to be an efficient catalyst for CO oxidation [9]. Therefore, in Au/CuO/ZnO catalysts, the undesired by-product CO formed even in small amount during POM through methanol decomposition and/or reverse water gas shift reactions is readily oxidized to carbon dioxide. Since Au/CuO/ZnO catalysts give higher hydrogen selectivity with negligible amount of CO compared to CuO/ZnO catalysts, a systematic study has been undertaken using Au/CuO/ZnO catalysts to optimize calcination temperature and reaction temperature for POM to produce hydrogen.

Fig. 5 shows the effect of calcination temperature on methanol conversion, hydrogen selectivity and carbon monoxide selectivity for partial oxidation of methanol at 523 K. All the catalysts show similar activity towards methanol conversion. As can be seen from the figure, methanol conversion is 100% and independent of reaction time. But it is clear that calcination conditions significantly influence the performance of the catalyst towards hydrogen formation. The hydrogen selectivity over Au/CuO/ZnO catalysts decreases in the following order: calcined at 573 K > calcined at 673 K > uncalcined. Thus, the optimum calcination temperature is 573 K. The lower activity of the uncalcined catalyst is due to the presence of hydrozincite as evidenced from XRD analysis (Fig. 1a). It was reported that the amount of active gold species available on the catalyst surface could be decreased in the presence of hydrozincite phase [26]. The lower activity of the catalyst at higher calcination temperatures (673 K) may be due to the presence of larger gold

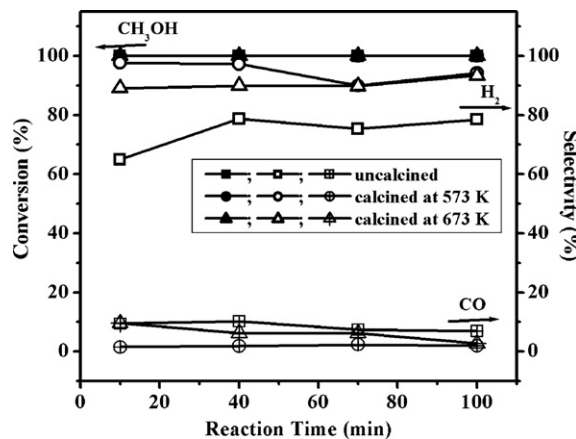


Fig. 5. Effect of calcination temperature on methanol conversion, hydrogen selectivity and carbon monoxide selectivity for partial oxidation of methanol over Au/CuO/ZnO catalysts (reaction temperature, 523 K).

and CuO particles. The mean particle size of gold increases from 3.4 to 4.6 nm and CuO size increases from 9.5 to 13 nm when the calcination temperature increases from 573 to 673 K (Fig. 2b and c). High temperature heating results in sintering of gold and copper particles and large particles are formed by coalesces of smaller particles. Highly dispersed Au particles are more active for methanol oxidation than for hydrogen oxidation, while large Au particles are more active for hydrogen oxidation [27]. The carbon monoxide selectivity over Au/CuO/ZnO catalysts decreases in the following order: uncalcined > calcined at 673 K > calcined at 573 K. The performance of the gold supported zinc oxide catalysts showed that the formation of hydrozincite led to the decrease in activity, because the interaction of CO and oxygen species might be suppressed by the carbonate-like species formed during reaction [12,14]. During POM, the carbon monoxide formed by methanol decomposition and/or reverse water gas shift (RWGS) is subsequently oxidized to carbon dioxide, since these catalysts are reported to be highly active for CO oxidation [9]. However, this process has been restricted by the presence of hydrozincite [26]. This causes formation of larger amount of carbon monoxide over the uncalcined catalyst sample. Moreover, for CO oxidation using supported gold catalysts, the particle size of gold plays an important role, smaller gold particles being highly active. Thus, the influence of the calcination effect on hydrogen selectivity depends on crystalline phases of support and particle size of Au present on the Au/CuO/ZnO catalysts. This leads to a conclusion that the Au/CuO/ZnO catalyst calcined at 573 K provides high hydrogen selectivity with low carbon monoxide selectivity. It is interesting to note that these catalysts are stable during catalytic tests. In our previous study on POM, we have inferred that the deactivation of Au/TiO<sub>2</sub> catalyst for hydrogen production is explained in terms of particle growth of Au during the course of the reaction [10]. In the present study, the Au particle size in the Au/CuO/ZnO catalyst increases from 3.4 to 5.4 nm after 2 h catalytic test (Fig. 2b and d). XRD analyses of the catalysts after reaction show the presence of new species Cu<sup>0</sup> (Fig. 1d). This can be interpreted to mean that CuO is reduced during the reaction. Metallic copper is reported as active species for the POM

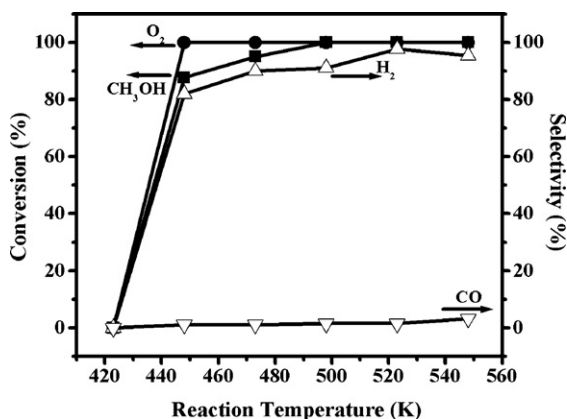
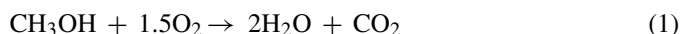


Fig. 6. Effect of reaction temperature on methanol conversion, oxygen conversion, hydrogen selectivity and carbon monoxide selectivity for partial oxidation of methanol over Au/CuO/ZnO catalysts (calcination temperature, 573 K; reaction time, 10 min).

reaction [3,12]. Therefore the Au/CuO/ZnO catalyst is considered as sustainable active catalyst for formation of hydrogen by POM.

The effect of reaction temperature on the catalytic performance of the Au/CuO/ZnO catalysts is depicted in Fig. 6. It can be observed that, the reaction sets on at 448 K. The O<sub>2</sub> conversion reaches 100% at 448 K, methanol conversion reaches 100% at 498 K and hydrogen selectivity reaches 97.7% at 523 K. CO selectivity is very low throughout the temperature range studied; the CO selectivity increases from 1.1 to 3.2%, when the reaction temperature increases from 448 to 548 K. The conversion and selectivity data illustrate the participation of several reactions during POM. During POM, methanol quickly consumes excess oxygen leading to highly exothermic methanol combustion (MC) reaction (Eq. (1)) to occur and produce water and carbon dioxide:



At 448 K, water selectivity was 18.1%. With increasing reaction temperature, water selectivity is decreased with consequent increase in hydrogen selectivity. This can be explained by assuming that water formed by MC is consumed by steam reforming of methanol (SRM) and produces hydrogen and carbon dioxide (Eq. (2)):



It is known that copper catalysts perform a variety of catalytic functions depending on its oxidation state. The metallic copper is active for SRM, while Cu<sup>2+</sup> as CuO promotes MC producing mainly water and carbon dioxide [7]. At low reaction temperature copper in Au/CuO/ZnO catalyst is present as copper oxide. With increasing reaction temperature some of the copper species are reduced to metallic copper. At 523 K, the selectivity towards hydrogen formation is 97.7%, which suggests that water is consumed by SRM. The SRM (Eq. (2)) can be considered as a combination of methanol decomposition (MD) (Eq. (3)) and water gas shift (WGS) (Eq. (4)):



According to this reaction sequence, if the entire CO formed in the MD is consumed in the WGS, coincidence in the proportion of products by SRM and by MD–WGS could be expected. The MD–WGS scheme has been proposed by several authors for SRM reaction over copper catalysts [28,29]. MD and reverse water gas shift (RWGS) (Eq. (5)) is believed to occur and produce CO when no more oxygen and water are available [5]:



Nevertheless, the CO selectivity is very low compared to that observed over supported Cu catalysts [3,4]. The CO formed by MD and RWGS can be converted to CO<sub>2</sub> by WGS (Eq. (4)) and/or by CO oxidation (Eq. (6)):



The presence of a certain proportion of CO in the reaction product at high temperature suggests that the rate of MD is high when the reaction temperature is above 523 K. It is important to note that, in the present study, complete conversion of methanol with very high hydrogen selectivity (97.7%) with small amount of carbon monoxide (~1.5%) is detected at 523 K. In our previous studies we have shown that a Au/TiO<sub>2</sub> catalyst produced a maximum of 35% hydrogen selectivity with 100% methanol conversion at 583 K and a Au/TiO<sub>2</sub>–Fe<sub>2</sub>O<sub>3</sub> catalyst produced 76% hydrogen selectivity with 95% methanol conversion at 548 K [10,11]. Therefore, the current results clearly indicate that improved catalytic performance can be achieved by using Au/CuO/ZnO catalysts for hydrogen production by partial oxidation of methanol.

#### 4. Conclusions

Production of hydrogen by partial oxidation of methanol was studied over Au/CuO/ZnO and CuO/ZnO catalysts. The Au/CuO/ZnO catalyst is more active and exhibited higher hydrogen selectively with smaller amount of CO than the CuO/ZnO catalysts. The enhanced activity of Au/CuO/ZnO catalyst is due to the strong interaction between Au and CuO species. The catalytic activity strongly depends on the calcination and reaction temperatures. The optimum calcination temperature for hydrogen selectivity is 573 K. The influence of calcination on the activity suggests that the activity depends on the crystalline phases of support and particle size of Au and CuO present on the catalysts. The effect of reaction temperature on the performance of the Au/CuO/ZnO catalysts was studied in the temperature range of 423–548 K. Both methanol conversion and hydrogen selectivity increase with increasing reaction temperature. Complete conversion of methanol is observed above 498 K. A high hydrogen selectivity of 97.7% with very low CO selectivity of 1.5% is observed at 523 K. The present study suggests that the Au/CuO/ZnO catalyst is an excellent catalyst for selective and effective production of hydrogen, making it possible to utilize this catalyst in the application of proton exchange membrane fuel cell.

## Acknowledgements

The authors express thanks to the Ministry of Economical Affairs of Taiwan for its financial support under contract number 93-EC-17-A-09-S1-022.

## References

- [1] B. Lindner, K. Sjomstrom, *Fuel* 63 (1984) 1485.
- [2] J. Appleby, F.R. Foulkes, *Fuel Cell Handbook*, Van Nostrand Reinhold, New York, 1989, p. 177.
- [3] L. Alejo, R. Lago, M.A. Peña, J.L.G. Fierro, *Appl. Catal. A* 162 (1997) 281.
- [4] J. Agrell, K. Hasselbo, K. Jansson, S.G. Järås, M. Boutonnet, *Appl. Catal. A* 211 (2001) 239.
- [5] J. Agrell, M. Boutonnet, J.L.G. Fierro, *Appl. Catal. A* 253 (2003) 213.
- [6] R.M. Navarro, M.A. Peña, J.L.G. Fierro, *J. Catal.* 212 (2002) 112.
- [7] J. Agrell, H. Birgersson, M. Boutonnet, I. Melián-Cabrera, R.M. Navarro, *J.L.G. Fierro, J. Catal.* 219 (2003) 389.
- [8] M. Haruta, N. Yamada, T. Kobayashi, S. Iijima, *J. Catal.* 15 (1989) 301.
- [9] G.J. Hutchings, M.R.H. Siddiqui, A. Burrows, C.J. Kiely, R. Whyman, *J. Chem. Soc., Faraday Trans.* 93 (1997) 187.
- [10] F.W. Chang, H.Y. Yu, L.S. Roselin, H.C. Yang, *Appl. Catal. A* 290 (2005) 138.
- [11] F.W. Chang, H.Y. Yu, L.S. Roselin, H.C. Yang, T.C. Ou, *Appl. Catal. A* 302 (2006) 157.
- [12] Z. Wang, W. Wang, G. Lu, *Int. J. Hydrogen Energy* 28 (2003) 151.
- [13] C.K. Chang, Y.J. Chen, C. Yeh, *Appl. Catal. A* 174 (1998) 13.
- [14] J. Zhang, Y. Wang, B. Chen, C. Li, D. Wu, X. Wang, *Energy Convers. Manage.* 44 (2003) 1805.
- [15] E.D. Guerreiro, O.F. Gorrioz, J.B. Rivarola, L.A. Arrfia, *Appl. Catal. A* 165 (1997) 259.
- [16] B. Lindström, L.J. Pettersson, P. Govind Menon, *Appl. Catal. A* 234 (2002) 111.
- [17] H. Oguchia, T. Nishiguchia, T. Matsumoto, H. Kanaia, K. Utania, Y. Matsumurab, S. Imamura, *Appl. Catal. A* 281 (2005) 69.
- [18] X. Fang, S. Yao, Z. Qing, F. Li, *Appl. Catal. A* 161 (1997) 129.
- [19] H.L. Lian, M.J. Jia, W.C. Pan, W.X. Zhang, D.Z. Jiang, *Chem. Res. Chin. U* 22 (2006) 99.
- [20] I.M. Cabrera, M.L. Granados, J.L.G. Fierro, *Catal. Lett.* 79 (2002) 165.
- [21] A. Venugopal, J. Aluha, D. Mogano, M.S. Scurrrell, *Appl. Catal. A* 245 (2003) 149.
- [22] S. Scirè, S. Minicò, C. Crisafulli, S. Ganvango, *Catal. Commun.* 2 (2001) 229.
- [23] S. Minicò, S. Scirè, C. Crisafulli, R. Maggiore, S. Ganvango, *Appl. Catal. B* 28 (2000) 245.
- [24] J. Agrell, M. Boutonnet, I.M. Cabrera, J.L.G. Fierro, *Appl. Catal. A* 253 (2003) 201.
- [25] D. Wang, Z. Haob, D. Chenga, X. Shi, C. Hu, *J. Mol. Catal. A* 200 (2003) 229.
- [26] G.Y. Wang, W.X. Zhang, H.L. Lian, D.Z. Jiang, T.H. Wu, *Appl. Catal. A* 239 (2003) 1.
- [27] T.V. Choudhary, C. Sivadinarayana, C.C. Chusuei, A.K. Datye, J.P. Fackler, D.W. Goodman, *J. Catal.* 207 (2002) 247.
- [28] J.C. Amphlett, R.F. Mann, R.D. Weir, *Can. J. Chem. Eng.* 66 (1988) 950.
- [29] E. Santacesaria, S. Carra, *Appl. Catal.* 5 (1983) 345.